

Theory of hyperfine interactions in alkaline-earth ions isoelectronic with alkali-metal atoms — $^{137}\text{Ba}^+$

S. Ahmad, J. Andriessen,* K. Raghunathan, and T. P. Das

Department of Physics, State University of New York, Albany, New York 12222

(Received 11 June 1981)

With the development of ion-storage techniques, it has become possible to study the hyperfine interactions of alkaline-earth positive ions which are isoelectronic with alkali-metal atoms. As part of a program to study the available experimental values of the hyperfine constants and the relative importance of various contributing mechanisms in these systems, we have investigated the singly ionized barium ion using relativistic many-body perturbation theory. The one-electron contribution to the hyperfine constant in $^{137}\text{Ba}^+$ is found to be 3476 MHz composed of direct and exchange core-polarization contributions of 3055 and 421 MHz, respectively. The many-electron correlation contribution is found to be 727 MHz. The net calculated hyperfine constant of (4203 ± 200) MHz agrees satisfactorily with the experimental value of 4018.2 MHz. The ratios of the exchange core-polarization and correlation contributions to the direct contribution are both found to be smaller than the corresponding ratios in the isoelectronic cesium atom. This can be ascribed to the lesser deformability of the core of Ba^+ as compared to that of the neutral cesium atom.

I. INTRODUCTION

With the development of ion-storage techniques¹, the hyperfine interaction data are becoming increasingly available in free ions with unpaired spin valence electrons. One of the interesting classes of free ion systems in which hyperfine data have recently become available² are the positive alkaline-earth ions. From a theoretical point of view, the understanding of the origin of the hyperfine interactions in these systems is of particular interest because they are isoelectronic with alkali atoms. The contributions to the hyperfine interactions in alkali atoms³ are well understood⁴ through the use of many-body perturbation-theoretic techniques⁵ including relativistic effects⁶ for the heavier atoms. Thus, interesting trends⁷ have been observed in the direct, exchange core polarization (ECP) and many-body correlation contributions in going from the lightest element, lithium, to the heaviest alkali, francium. The direct contribution to the hyperfine field at the nucleus appears to be nearly constant over the whole series, while the ECP contribution as a fraction of the direct contribution decreases rapidly from lithium to sodium, and then much

more gradually as one proceeds to francium. The correlation contribution, on the other hand, shows a marked increase in importance in going from lithium to the heavier atoms, leveling off around rubidium and cesium, and decreasing in importance on going to francium. Physical reasons for these trends have been proposed in the literature.⁸ One expects to enhance the physical understanding of these trends and of the mechanisms contributing to the hyperfine interaction by studying the closely related positive ions of the alkaline-earth series. We are engaged in a systematic investigation of this series starting with one of the heavier alkaline-earth ions, $^{137}\text{Ba}^+$, for which experimental hyperfine data are available. The aims of our investigation as far as this specific ion is concerned were twofold, namely, to attempt to explain quantitatively the net observed hyperfine constant and secondly to compare the contributions to the hyperfine field in this ion with the isoelectronic cesium atom⁹ to study how the extra charge in Ba^+ influences both the absolute values of the direct, ECP, and correlation contributions as well as their relative importance with respect to each other.

In Sec. II, we present a brief description of the

relativistic many-body procedure employed in this work, as more detailed descriptions are available in the literature for other atoms^{5,6} including the alkali atoms.⁴ However, for the sake of completeness, a few details of the potential and basis sets for the evaluation of the perturbation diagrams, pertinent to the present system, are included. Important diagrams describing the physical mechanisms contributing to the hyperfine interaction are also presented in this section. Section III presents the contributions from various diagrams, with appropriate combinations of these to obtain the contributions associated with various physical mechanisms. Comparisons with cesium and other alkali atoms and discussions are also included in this section. Section IV lists the main conclusions of our work and its implications for other ions of the alkaline-earth series.

II. THEORY AND PROCEDURE

The relativistic many-body perturbation theory (RMBPT) adopted in the present work has been described in detail in a number of earlier papers,⁶ including a recent one on the ground state of the alkali atom, rubidium.¹⁰ A few of the important points of the procedure will be given here, both for the sake of completeness and because they apply specifically to the system Ba⁺ under consideration.

The many-electron relativistic Hamiltonian for an atom with nuclear charge Z is given by⁶

$$\mathcal{H} = c \sum_i \vec{\alpha}_i \cdot \vec{p}_i + \sum_i \beta_i mc^2 - \sum_i \frac{Ze^2}{r_i} + \sum_{i>j} \frac{e^2}{r_{ij}}, \quad (1)$$

where $\vec{\alpha}_i$ and β_i are Dirac matrices, e and m electronic charge and mass, \vec{r}_i and \vec{p}_i are, respectively, the position (with respect to nucleus) and momentum vectors of the i th electron. r_{ij} represents the distance between electrons i and j .

To obtain the exact expectation value of any operator O for the atom under study, we need the exact many-electron eigenfunction Ψ_0 of \mathcal{H} given by

$$\mathcal{H}\Psi_0 = E\Psi_0. \quad (2)$$

However, since the exact solution cannot be obtained in a straightforward manner, we take recourse to a perturbation procedure in which one starts with the eigenfunction Φ_0 of an approximate Hamiltonian \mathcal{H}_0 , satisfying the equation

$$\mathcal{H}_0\Phi_0 = E_0\Phi_0, \quad (3)$$

and uses various orders in the perturbation Hamiltonian

$$\mathcal{H}' = \mathcal{H} - \mathcal{H}_0 \quad (4)$$

to correct the expectation value over Φ_0 . With this formalism, one gets the linked cluster expansion

$$\begin{aligned} \langle \mathcal{H}'_N \rangle &= \frac{\langle \Psi_0 | \mathcal{H}'_N | \Psi_0 \rangle}{\langle \Psi_0 | \Psi_0 \rangle} \\ &= \sum_{m,n}^L \langle \Phi_0 \left| \left[\frac{\mathcal{H}'}{E_0 - \mathcal{H}_0} \right]^m \right. \\ &\quad \left. \times \mathcal{H}'_N \left[\frac{\mathcal{H}'}{E_0 - \mathcal{H}_0} \right]^n \right| \Phi_0 \rangle, \end{aligned} \quad (5)$$

where m and n , in principle, run over all orders of perturbation. For the zero-order Hamiltonian \mathcal{H}_0 , the $V^{(N-1)}$ approximation to the potential has been found to be the most convenient for the study of atomic properties,⁴⁻⁶ the relativistic form for \mathcal{H}_0 in this approximation being given by

$$\mathcal{H}_0 = c \sum_i \vec{\alpha}_i \cdot \vec{p}_i + \sum_i \beta_i mc^2 - \sum_i \frac{Ze^2}{r_i} + \sum_i V_i^{(N-1)}. \quad (6)$$

The matrix element of the V^{N-1} potential over one-electron states is given by

$$\begin{aligned} \langle a | V^{N-1} | b \rangle &= \sum_{n=1}^{N-1} \left\langle \left\langle an \left| \frac{1}{r_{12}} \right| bn \right\rangle \right. \\ &\quad \left. - \left\langle an \left| \frac{1}{r_{12}} \right| nb \right\rangle \right\}, \end{aligned} \quad (7)$$

the summation over n being taken over all the occupied states of the atom except one that is excluded, a common choice for this excluded state being the outermost valence state. In the present work we have chosen the outermost $6s_{1/2}$ state as the one excluded in the summation in Eq. (7). With this choice of the one-electron potential, the perturbation \mathcal{H}' is given by

$$\mathcal{H}' = \sum_{i>j} \frac{e^2}{r_{ij}} - \sum_i V_i^{N-1}. \quad (8)$$

For the construction of the zero-order many-electron state Φ_0 and the excited many-electron states needed for evaluating the perturbation sum in Eq. (5), one needs to obtain the complete set of one-electron states which are solutions of the one-electron Dirac equation

$$\left[c \vec{\alpha} \cdot \vec{p} + \beta mc^2 - \frac{Ze^2}{r} + V^{N-1} \right] \phi_n = \epsilon_n \phi_n. \quad (9)$$

The procedure for solving these equations for both discrete and continuum states are described in the literature⁴⁻⁶ and shall not be dealt with here. The actual equations that are solved are the radial counterparts of Eq. (9) which yield the large and small component¹¹ radial functions P_n and Q_n corresponding to ϕ_n .

Before proceeding to the many-body diagrams resulting from the perturbation series in Eq. (5), we would like to discuss the form¹² of the hyperfine Hamiltonian and expression for the hyperfine constant A that occurs in the spin Hamiltonian for the atom. This is the experimental quantity which the theory has to explain. In relativistic theory the hyperfine Hamiltonian \mathcal{H}'_N is given by

$$\mathcal{H}'_N = ec \sum_i \vec{r}_i \cdot \left[\frac{\vec{\mu}_N \times \vec{r}_i}{r_i^3} \right], \quad (10)$$

where $\vec{\mu}_N$ is the nuclear moment. The spin-Hamiltonian term \mathcal{H}'_S used to describe the hyperfine splitting of the optical or Zeeman levels of the atom in a magnetic field is given by

$$\mathcal{H}'_S = A \vec{I} \cdot \vec{J}, \quad (11)$$

where \vec{I} is the nuclear spin and \vec{J} is the total angular momentum of the electron. The expression for A in terms of the expectation value of \mathcal{H}'_N over the exact many-electron wave function Ψ_J is given by

$$A = \frac{1}{IJ} \langle \Psi_J | \mathcal{H}'_N | \Psi_J \rangle, \quad (12)$$

where Ψ_J refers to the exact many-electron wave function with magnetic quantum number $M_J = J$. Using the perturbation expansion (5) for the expectation value in Eq. (12), we get

$$A = \frac{1}{IJ} \sum_{m,n} \langle \Phi_J \left| \left[\frac{\mathcal{H}'_N}{E_0 - \mathcal{H}_0} \right]^m \times \left[\frac{\mathcal{H}'_N}{E_0 - \mathcal{H}_0} \right]^n \right| \Phi_J \rangle, \quad (13)$$

where Φ_J is the zero-order many-electron wave function with $M_J = J$. As is usual in RMBPT, the indices m and n define the orders of the perturbation diagrams contributing to A . Thus the lowest order (zero-order) diagram resulting from $m = n = 0$ is referred to as (0,0); the first-order diagrams are referred to as (0,1), while second-order diagrams can be either of the form (1,1) or (0,2).

Previous investigations on the alkali-metal atom



FIG. 1. (0,0) direct diagram.

series⁴ have shown that in all cases, the (0,0), (0,1), and (0,2) diagrams shown in Figs. 1, 2, and 3 make almost the entire contribution (more than 97%) to A . The (0,0) diagram represents the direct contribution from the valence 6s electron and is the only contribution that occurs in the restricted Hartree-Fock approximation where the core states differ only in spin. The (0,1) diagram represents the exchange core-polarization (ECP) effect where the core state with spin parallel to the valence electron is subjected to the exchange potential from the latter. The hole states being perturbed in the diagram of Fig. 2 are only the s states in nonrelativistic theory, but can also be p states in relativistic theory.¹⁰ However, the latter have been found to contribute very little in alkali-metal atoms. The (0,2) diagram represents the major correlation effect arising from the mutual dynamic excitations of the valence 6s electron and other core electrons, however in alkali-metal atoms the main correlation contribution arises from the outermost core electrons only. In addition to the diagram in Fig. 3 there are other second-order, (1,1), and (0,2) diagrams as well as higher order diagrams which are rather time consuming to evaluate and are also expected to be small. Such diagrams were explicitly evaluated in the case of alkali-metal atoms⁴ and were found to be insignificant. Therefore rather than considering these diagrams explicitly, in the present work we have evaluated only a few of them to verify their smallness and an estimated value based on previous investigations has been assumed while quoting the final results.

III. RESULTS AND DISCUSSION

There are two barium isotopes available in nature, namely, ¹³⁵Ba and ¹³⁷Ba. The result presented

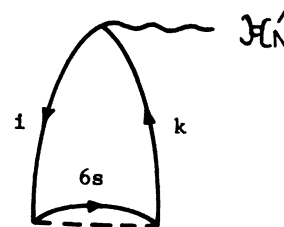


FIG. 2. Exchange core polarization or (0,1) diagram.

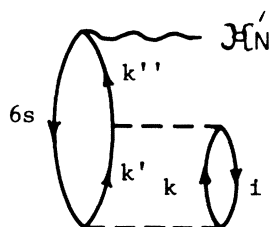


FIG. 3. Typical (0,2) direct diagram making the major correlation contribution.

here corresponds to ^{137}Ba , which has a magnetic moment¹³ $\mu_{137} = 0.935$ nuclear magneton and spin $I = \frac{3}{2}$. To obtain the corresponding results for ^{135}Ba one has to multiply the ^{137}Ba results by $\mu_{135}/\mu_{137} = 0.895$, as both the isotopes have the same spin.

Contributions from various mechanisms that contribute to the hyperfine constant A are listed in Table I. We wish to discuss the correlation contributions first. There are a number of diagrams⁴ that contribute to the major correlation effect. The important ones belong to the families represented by Figs. 3 and 4. The diagrams represented by Fig. 3 with $i = 5p, 5s,$ and $4d$ describe the influence of mutual correlations of each of these three outermost core shells with the $6s$ valence electron. We have evaluated the contributions to diagram 3 from multipoles 0 and 1 in the expansion of $1/r_{12}$ as well as from higher multipoles. As seen from Table II, $l=0$ and 1 make the major contribution, although that from the rest of the multipoles is by no means negligible. Contributions from inner shells have been neglected because they are expected to be small.^{4,8} The diagrams typified by Fig. 4

TABLE I. Contributions from different mechanisms to the hyperfine constant A .

Mechanism	Contribution (MHz)
Zero order (Fig. 1)	3055.0
Exchange core polarization (Fig. 2)	421.1
Major (0,2) correlation (Fig. 3)	913.6
Other second-order correlations	-225.7
Higher-order correlation	38.8
Net correlation	726.7
Total	(4203 ± 200)
Experimental ^a	4018.2

^aBecker *et al.* in Ref. 2.

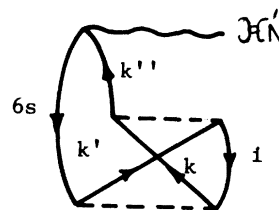


FIG. 4. Major (0,2) exchange correlation diagram.

are the exchange counterparts of those represented by Fig. 3. They have been explicitly evaluated for i corresponding to $5p, 4d,$ and $5s$ core shells.

Table II lists the contributions from direct and exchange correlation effects associated with the $5p, 4d,$ and $5s$ shells. Contributions from the corresponding diagrams listed in Table II indicate trends very similar to those in the alkali atoms.^{4,8-10} Thus, for monopole and dipole excitations, the correlation effect associated with the $5p$ shell is the dominant one, while the $4d,$ and $5s$ contributions are found in decreasing order — a feature similar to that observed in rubidium⁹ and cesium.¹⁰ Also, interestingly, it is noted that the ratios of diagrams like, for example, case (b) and case (a) for Fig. 3 are very close to those for the neutral alkali-metal atoms. This feature has also been found in rubidium,¹⁰ cesium,⁹ and francium.⁸ This observation is indicative of the interesting fact that while the deformabilities of different shells starting with the valence and outermost cores may all change in going from one alkali-metal atom (or alkaline earth ion) to another, the deformabilities of the shells in each atom, relative to each other, remain the same. This observation is useful because it allows us to estimate correlation effects for other diagrams not presented in Table II.

As can be seen from Table II, the quadrupolar and higher order multipole contributions are significantly smaller than the net contributions from the monopole and dipole effects for both $5p$ and $4d$ shells, but larger for the $5s$ shell. Both these trends have also been observed in neutral alkali-metal atoms.^{9,10} Finally, exchange correlation contributions from diagrams of type shown in Fig. 4 have been evaluated for multipole excitations from monopole through octopole for $5p, 4d,$ and $5s$ shells and, while they are all significant in size, they are considerably smaller than the direct correlation contributions listed in Table II.

Returning to Table I, the first three rows correspond to the contributions from the direct, ECP,

TABLE II. Individual contributions from major correlation diagrams.

Mechanism	Contribution (MHz)
<i>5p</i> correlation mechanism	
Diagram 3, Case (a) $i = 5p, k = kd, k' = k'p, k'' = k''s$	448.9
Case (b) $i = 5p, k = ks, k' = k'p, k'' = k''s$	4.7
Case (c) $i = 5p, k = kp, k' = k's, k'' = k''s$	91.4
Net <i>5p</i> correlation contribution from monopole and dipole excitations	545.0
Net <i>5p</i> correlation contribution from quadrupole and higher-order excitations	205.6
Total <i>5p</i> correlation contribution	750.6
<i>4d</i> correlation mechanism	
Diagram 3, Case (d) $i = 4d, k = kf, k' = k'p, k'' = k''s$	97.6
Case (e) $i = 4d, k = kp, k' = k'p, k'' = k''s$	3.1
Case (f) $i = 4d, k = kd, k' = k's, k'' = k''s$	43.4
Net <i>4d</i> correlation contribution from monopole and dipole excitations	144.1
Net <i>4d</i> higher-order excitations	40.1
Total <i>4d</i> correlation contribution	184.2
<i>5s</i> correlation mechanism	
Diagram 3, Case (g) $i = 5s, k = kp, k' = k'p, k'' = k''s$	10.3
Case (h) $i = 5s, k = ks, k' = k's, k'' = k''s$	16.5
Net <i>5s</i> correlation contribution from monopole and dipole excitations	26.8
Net <i>5s</i> higher-order excitations	63.9
Total <i>5s</i> correlation contribution	90.7
Net (0,2) contribution from diagrams typified by Fig. 3	1025.5
exchange correlation contribution from <i>5p</i>	-67.3
exchange correlation contribution from <i>4d</i>	-16.3
exchange correlation contribution from <i>5s</i>	-28.3
net (0,2) exchange contribution from diagrams of type (4)	-111.9
net (0,2) major correlation contribution	913.6

and the correlation mechanisms, the correlation contributions being the net result of major diagrams listed in Table II. As mentioned before, in addition to these second-order diagrams, there are a large number of other second-order and higher-order diagrams contributing to this effect. These diagrams have not been evaluated explicitly, rather they have been estimated from the results in rubidium^{8,10} using the near constancy of ratios of correlation diagrams observed in different alkali-metal atoms and the present system, as discussed earlier.

The next two entries in Table I correspond to these estimated values. The net correlation contribution, combining those from the major diagrams we have explicitly evaluated and the second and higher order diagrams which have been estimated, is given in the sixth row. We have ascribed a confidence limit of 200 MHz to the calculated value of the total hyperfine constant taking into account the possible uncertainties associated with the estimations we have made of some of the correlation diagrams and the accuracy of our computational procedures.

Within this confidence limit, the agreement with the experimental result is found to be good.¹⁴

IV. CONCLUSIONS

The good agreement obtained between theory and experiment gives indirect support to the values we have obtained for the individual contributions, direct, ECP, and correlation, and to the conclusions we draw about their relative trend as compared to the isoelectronic alkali-metal atoms. Thus, we observe that the ratios of the ECP and correlation effects to direct contributions in Ba^+ are about 14% and 24%, respectively, as compared to about 17% and 37% for cesium⁹ and 20% and

31% for rubidium.¹⁰ The relatively weaker contributions for both ECP and correlation effects are in keeping with physical expectations because the cores of Ba^+ are less deformable than the corresponding isoelectronic neutral alkali-metal atoms. It would be interesting to study the trend in these effects in going from the light alkaline-earth ions like Mg^+ to relatively heavier like Ba^+ , to see how they compare with the corresponding trends in the alkali-metal atom series. More information on this trend is expected in the future from many-body investigations on Mg^+ in which ²⁵Mg hyperfine data have recently become available.¹⁵

This work was partially supported by Grant No. GM 25230 from the National Institutes of Health.

*Permanent address: Technische Natuurkunde, Technische Hogeschool, Delft, Netherlands.

¹D. J. Wineland and H. G. Dehmelt, *J. App. Phys.* **46**, 919 (1975); W. Neuhauser, M. Hohenstatt, P. Toschek, and H. Dehmelt, *Phys. Rev. Lett.* **41**, 233 (1978); D. J. Wineland, J. C. Bergquist, W. M. Itano, and R. E. Drullinger, *Opt. Lett.* **5**, 245 (1980).

²W. M. Itano, D. J. Wineland, R. E. Drullinger, and J. C. Bergquist, *Abstracts of the Seventh International Conference on Atomic Physics* (MIT, Cambridge, Mass., 1980), p.238; W. M. Itano and D. J. Wineland (unpublished); W. Becker, W. Fischer, and H. Huhnermann, *Z. Phys.* **216**, 142 (1968); C. Hohle, H. Huhnermann, Th. Meier, and H. Wagner, *Z. Phys. A* **284**, 261 (1978).

³*Hyperfine Interactions*, edited by A. J. Freeman and R. B. Frankel (Academic, New York, 1967); H. Kopfermann, *Nuclear Moments* (Academic, New York, 1958); S. Penselin, T. Moran, V. W. Cohen, and G. Winkler, *Phys. Rev.* **127**, 524 (1962); G. H. Fuller and V. W. Cohen, *Nucl. Data Sec. A* **5**, 443 (1969).

⁴E. S. Chang, R. T. Pu, and T. P. Das, *Phys. Rev.* **174**, 1 (1968); T. Lee, N. C. Dutta, and T. P. Das, *Phys. Rev. A* **1**, 995 (1970); M. Vajed-Samii, J. Andriessen, S. N. Ray, B. P. Das, and T. P. Das, *Bull. Am. Phys.*

Soc. **25**, 397 (1980); B. P. Das, S. N. Ray, T. Lee, and T. P. Das, *Bull. Am. Phys. Soc.* **24**, 477 (1979); I. Lindgren and A. Rosen, *Case Stud. At. Phys.* **4**, (1974).

⁵N. C. Dutta, C. Matsubara, R. T. Pu, and T. P. Das, *Phys. Rev. Lett.* **21**, 1139 (1968).

⁶J. Andriessen, K. Raghunathan, S. N. Ray, and T. P. Das, *Phys. Rev. B* **15**, 2533 (1977).

⁷M. Vajed-Samii, B. P. Das, and T. P. Das, *Bull. Am. Phys. Soc.* **25**, 397 (1981).

⁸M. Vajed-Samii, Ph.D. thesis, State University of New York at Albany, 1980 (unpublished).

⁹B. P. Das *et al.* in Ref. 4.

¹⁰M. Vajed-Samii, S. N. Ray, T. P. Das, and J. Andriessen, *Phys. Rev. A* **20**, 1787 (1979); M. Vajed-Samii *et al.* in Ref. 4.

¹¹H. A. Bethe and E. E. Salpeter, *Quantum Mechanics of One and Two-Electron Atoms* (Plenum/Rosetta, New York, 1977).

¹²T. P. Das, *Relativistic Quantum Mechanics of Electrons* (Harper and Row, New York, 1973); I. Lindren and A. Rosen in Ref. 4.

¹³R. H. Hay, *Phys. Rev.* **60**, 75 (1941).

¹⁴W. Becker *et al.* in Ref. 2.

¹⁵W. M. Itano *et al.* in Ref. 2.